Smart Structures and Systems, Vol. 6, No. 8 (2010) 889-903
DOI: http://dx.doi.org/10.12989/sss.2010.6.8.889

Nonlinear dynamic response and its control of rubber components with piezoelectric patches/layers using finite element method

M.C. Manna*[1], R. Bhattacharyya[2] and A.H. Sheikh[3]

[1]*Department of Aerospace Engineering and Applied Mechanics, Bengal Engineering and Science University, Shibpur, Howrah - 711 103, India*
[2]*Department of Mechanical Engineering, Indian Institute of Technology, Kharagpur - 721 302, India*
[3]*Department of Civil, Environmental and Mining Engineering, University of Adelaide, SA - 5005, Australia*

(Received March 6, 2009, Accepted October 27, 2009)

Abstract. Idea of using piezoelectric materials with flexible structures made of rubber-like materials is quite novel. In this study a non-linear finite element model based on updated Lagrangian (UL) approach has been developed for dynamic response and its control of rubber-elastic material with surface-bonded PVDF patches/layers. A compressible stain energy density function has been used for the modeling of the rubber component. The results obtained are compared with available analytical solutions and other published results in some cases. Some results are reported as new results which will be useful for future references since the number of published results is not sufficient.

Keywords: nonlinear finite element; compressible strain energy function; hyperelastic material; piezoelectric material; dynamic response; smart rubber beam.

1. Introduction

The use of rubber as strategic structural material is gaining popularity steadily due to some of its specific features. One of the significant advantages of the material is its ability to dissipate kinetic energy associated with impact, shock or any form of dynamic loading, which is much higher compared to other materials. The material has extremely large amount of deformability and interesting it retains elasticity in that range of deformation if Mullin's effect and permanent set are ignored. These unique features are exploited to solve many engineering problems in an elegant manner. The use of rubber as vibration isolators, shock absorbers, load bearing materials, sealant materials and filler materials between two railway lines are some of its important applications. This specific aspect is well documented in the text by Gent (2001).

Discovery of the piezoelectric materials by the Curie brothers in the 1880s has opened a new area of research and one of its fruitful applications is found in the control or suppress of vibration of structures. In a piezoelectric material, electric charge is produced due to direct piezoelectric effect when it is subjected to a mechanical deformation and it gets deformed when a polarity is applied to

*Corresponding author, Associate Professor, E-mail: mcmbecdu@lycos.com

it through a differential voltage by virtue of converse piezoelectric effect. Initially the utilization of piezoelectric materials was made in the field of ultrasonics. Later the advantage of these unique properties has been successfully engineered in different fields of science and technology in early 1900's. In the present context, the contributions of Olson (1956) Allik and Hughes (1970) and Forward (1979) have deserved well mentioning. The use of a thin poly vinylidene fluoride (PVDF) layer was first proposed by Bailey and Hubbard (1985) for having additional damping in thin beams. By this time numbers of investigations have been carried out to study the effect of integrated piezoelectric layers or patches on the behaviour of different structures under different modes (Fanson and Caughey 1987, Crawley and de Luis 1987, Park and Chopra 1996).

Samanta *et al*. (1996) presented a generalized finite element formulation for active vibration control of a laminated plate integrated with piezoelectric polymer layers acting as distributed sensors and actuators using a two-dimensional eight-node quadrilateral isoparametric element with the help of higher order shear deformation theory. Chen *et al*. (1997) proposed a linear finite element formulation for vibration analysis and its suppression of intelligent structures. Ray *et al*. (1998) have extended their previous analytical model (Ray *et al*. 1993) to study the dynamic analysis of smart laminated plates. They have presented the exact expressions of the mechanical displacements, stresses, electrical displacements and potential for dynamic response of composite plates with piezoelectric layers bonded at the top and bottom surfaces. They have shown that the results obtained by their analytical solutions have good agreement with those obtained by their finite element analysis (Ray *et al*. 1994).

Gaudenzi *et al*. (2000) studied active vibration control of a cantilever beam made of aluminium for the attenuation of vibration effects by two approaches – position and velocity control. They validated their numerical model with experimental data. A nonlinear finite element analysis of composite structures such as beams and plates integrated with piezoelectric material has been proposed by Ye *et al*. (2000) using Updated Lagrangian approach. Lim *et al.* (2001) have conducted a three-dimensional analytical study for a parallel piezoelectric bimorph used as sensor as well as actuator utilizing state space formulation combined with an asymptotic expansion technique.

Thornburgh *et al*. (2004) have derived an analytical model for smart structures and applied to determine the transient dynamic response of arbitrary structures with piezoelectric materials. The equations of motion have been obtained from a coupled piezoelectric-mechanical formulation. They compared the results predicted by the higher-order laminate theory and the classical plate theory and similarly the results predicted by the coupled and uncoupled piezoelectric models. The analysis is confined to composite structures with surface bonded PZT materials only. Lee *et al*. (2004) have studied the vibration control of transient dynamic response of laminated composite plates with integrated smart material layers as sensors and actuators. They have used a unified plate theory that includes classical, first-order and third-order plate theories as special cases.

Chattopadhyay *et al*. (2004) have proposed a nonlinear vibration analysis procedure to investigate the dynamic response of composite laminates with embedded and/or surface bonded piezoelectric sensors having multiple finite/discrete delaminations. A refined layerwise plate theory has been used to develop the piezoelectric-mechanical model for accurate prediction of the sensor voltage output in the time domain analysis. Mukherjee and Chaudhuri (2004) have used displacement feedback control and velocity feedback control technique to explain a comprehensive formulation for instability control of piezolaminated imperfect struts made of steel and PZT layers using an imperfect approach under arbitrary dynamic excitation. In this context, the study of Mukherjee and Chaudhuri (2005a) is worth mentioning where the exact solutions have been presented along with

experimental results to show the effect of axial forces on smart columns made of plastic substrates and PVDF layers. They (2005b) have also studied the nonlinear dynamic response of piezolaminated smart beams made of PVDF layers. However, all these studies are limited to structures made of piezoelectric materials with conventional isotropic elastic materials.

The concept of using piezoelectric layers/patches integrated with a structural component made of rubber is quite novel. So far the number of investigations carried out on this problem is very few (Austin and Ananthasayanam 2002) but it has potential future applications, as rubber is steadily gaining popularity in its use in various engineering problems. The modeling of is problem is quite challenging, as rubber is a hyperelastic material having near incompressible behaviour and it often undergoes an extremely large deformation, which leads to severe geometric nonlinearity. The mechanical properties of rubber are characterized by a suitable strain energy density function, which results in nonlinear stress-strain relationship. These are responsible for making the mathematical model of piezolaminated rubber quite complex and it can be expected that the finite element model of the problem would be an arduous task. In the study of Austin and Ananthasayanam (2002), an attempted has been made to investigate the effect of piezoelectric patches on curvatures of the rubber substrate due to application of actuating voltage. They concentrated their attention only on linear static analysis of the structure. So a very limited information are available on the effect of surface bonded piezoelectric patches/layers on the behaviour of rubber-like structural components under static and dynamic loading. Keeping this aspect in view an attempt has been made in the present study to develop a displacement based nonlinear finite element method for predicting the dynamic response and its control of flexible structures made of rubber and the piezoelectric layers (PVDF). The focus of the present study is to understand the piezoelectric effect on dynamic response and its control of rubber components considering geometric non-linearity for both rubber and piezoelectric materials and material non-linearity for rubber material.

2. Finite element formulation

The incremental-iterative solution technique is most suitable for dynamic analysis of a smart rubber component, as it involves severe nonlinearity in such analysis. In this solution scheme, the entire path of deformation is divided into a number of time steps. It gives different configurations/ states such as ${}^{0}\Pi$, …., ${}^{t}\Pi$, ${}^{t+\Delta t}\Pi$, …., where ${}^{0}\Pi$ is the initial state while ${}^{t}\Pi$ is any intermediate one. In this system any displacement component and the electric potential at two adjacent states of deformations may be expressed as

$$ {}^{t+\Delta t}u_i = {}^{t}u_i + u_i \quad (i = 1, 2 \text{ and } 3), \qquad {}^{t+\Delta t}\varphi = {}^{t}\varphi + \varphi \tag{1} $$

where u_i and φ are the increment of the displacement component ${}^{t}u_i$ and the electric potential ${}^{t}\varphi$, respectively. In a similar manner the co-ordinates at any state may be expressed as

$$ {}^{t+\Delta t}x_i = {}^{0}x_i + {}^{t+\Delta t}u_i \quad \text{or} \quad {}^{t+\Delta t}x_i = {}^{t}x_i + u_i \tag{2} $$

Now the equilibrium equation of the body at any instant of time may be obtained using the principle of virtual work and it may be expressed according to Updated Lagrangian technique (Bathe 1996) as

$$\int \delta({}^{t+\Delta t}_{t}\varepsilon)\, {}^{t+\Delta t}_{t}\sigma\, {}^{t}dV = {}^{t+\Delta t}P \tag{3}$$

where

$${}^{t+\Delta t}P = \int \delta({}^{t+\Delta t}u_k)\, {}^{t}\rho({}^{t+\Delta t}_{t}f_k)\, {}^{t}dV + \int \{\delta({}^{t+\Delta t}u_k)\, {}^{t+\Delta t}_{t}t_k + \delta({}^{t+\Delta t}\phi)\, {}^{t+\Delta t}_{t}Q\}\, {}^{t}dA \tag{4}$$

In the above Eqs. (3) and (4), $\delta({}^{t+\Delta t}_{t}\varepsilon)$ is the variation of Green-Lagrangian strain ${}^{t+\Delta t}_{t}\varepsilon$, ${}^{t+\Delta t}_{t}\sigma$, is the corresponding 2nd Piola Kirchhoff stress, ${}^{t}dV$ is the volume of an element, ${}^{t}\rho$ is the density at instant t, ${}^{t+\Delta t}_{t}f_k$ is the body force per unit mass, ${}^{t+\Delta t}_{t}t_k$ is the deformation independent surface force, ${}^{t+\Delta t}_{t}Q$ is the surface charge and ${}^{t}dA$ is the surface area of an element at instant t. The left superscript denotes the configuration at instant $(t+\Delta t)$ where the quantity is considered whereas the left subscript denotes the configuration at instant t and the quantity is measured with respect to this configuration.

Now the abovementioned generalized stress and strain may be expressed with the help of incremental decomposition as follows

$${}^{t+\Delta t}_{t}\sigma = {}^{t}_{t}\sigma + \sigma \tag{5}$$

and

$${}^{t+\Delta t}_{t}\varepsilon_{ij} = {}^{t}_{t}\varepsilon + \varepsilon \tag{6}$$

Since ${}^{t}_{t}\varepsilon = 0$ in the above equation, it may be expressed by splitting the incremental part ε into linear and nonlinear components as

$${}^{t+\Delta t}_{t}\varepsilon = \varepsilon = \varepsilon^{0} + \varepsilon^{L} \tag{7}$$

where $\varepsilon^{0}, \varepsilon^{L}, \varepsilon^{0}_{ij}, E_i$ and ε^{L}_{ij} are explained in Manna *et al.* (2009).

Again ${}^{t}_{t}\sigma$ is simply the generalized Cauchy stress ${}^{t}\tau$ and with this, Eq. (5) becomes

$${}^{t+\Delta t}_{t}\sigma = {}^{t}\tau + \sigma \tag{8}$$

The generalized Cauchy stress ${}^{t}\tau$ and the incremental stress σ with corresponding electric components in the above equation may be expressed as (Manna *et al*. 2009)

$$\begin{Bmatrix} \{{}^{t}\tau\} \\ \{{}^{t}D\} \end{Bmatrix} = \begin{bmatrix} {}_{t}\hat{C} & {}_{t}\hat{e} \\ {}_{t}\hat{e}^{T} & -{}_{t}\hat{L} \end{bmatrix} \begin{Bmatrix} \{{}^{t}\varepsilon\} \\ \{{}^{t}E\} \end{Bmatrix} = [{}_{t}\overline{C}]\{{}^{t}\varepsilon\} \tag{9}$$

$$\begin{Bmatrix} \{\sigma\} \\ \{D\} \end{Bmatrix} = \begin{bmatrix} {}_{t}\hat{C} & {}_{t}\hat{e} \\ {}_{t}\hat{e}^{T} & -{}_{t}\hat{L} \end{bmatrix} \begin{Bmatrix} \{\varepsilon\} \\ \{E\} \end{Bmatrix} = [{}_{t}\overline{C}]\{\varepsilon\} \tag{10}$$

With the help of the above equations, Eq. (3) becomes

$$\int \delta(\varepsilon)_{t}\overline{C}\varepsilon\, {}^{t}dV + \int \delta(\varepsilon^{L})\, {}^{t}\tau\, {}^{t}dV = {}^{t+\Delta t}P - \int \delta(\varepsilon^{0})\, {}^{t}\tau\, {}^{t}dV \tag{11}$$

Since it is not possible to solve the above equation due to the presence of nonlinear incremental strains, it is linearized (Bathe 1996) by taking $\delta(\varepsilon) = \delta(\varepsilon^0)$ and $\varepsilon = \varepsilon^0$ to get an approximate solution. With these the Eq. (11) becomes

$$\int \delta(\varepsilon^0)_t \overline{C} \varepsilon^0 {}^t dV + \int \delta(\varepsilon^L)^t \tau \, {}^t dV = {}^{t+\Delta t}P - \int \delta(\varepsilon^0)^t \tau \, {}^t dV \tag{12}$$

Since $\delta({}^{t+\Delta t}u_k) = \delta(u_k)$ and $\delta({}^{t+\Delta t}\phi) = \delta(\phi)$, the virtual work due to external loads ${}^{t+\Delta t}P$ presented in Eq. (4) may be rewritten as

$${}^{t+\Delta t}P = \int \delta(u_k)^t \rho({}^{t+\Delta t}_t f_k) \, {}^t dV + \int \{ \delta(u_k)^{t+\Delta t}_t t_k + \delta(\phi)^{t+\Delta t}_t Q \} \, {}^t dA \tag{13}$$

Eqs. (12) and (13) may be expressed (Manna *et al.* 2009) as

$$\begin{aligned} &\int \delta\{\varepsilon^0\}^T [{}_t\overline{C}] \{\varepsilon^0\} \, {}^t dV + \int \delta(\theta)^T [{}^t\overline{\tau}] \{\theta\} \, {}^t dV \\ &= {}^{t+\Delta t}P - \int \delta\{\varepsilon^0\}^T \{{}^t\tau\} \, {}^t dV \end{aligned} \tag{14}$$

and

$${}^{t+\Delta t}P = \int \delta\{\overline{u}\}^T {}^t \rho \{{}^{t+\Delta t}_t \overline{f}\} \, {}^t dV + \int (\delta\{\overline{u}\}^T \{{}^{t+\Delta t}_t \overline{t}\} + \delta(\phi)^{t+\Delta t}_t Q) \, {}^t dA \tag{15}$$

where the different matrices in the above Eqs. (14) and (15) are explained in Manna *et al.* (2009).

Now Eqs. (14) and (15) are in convenient form for finite element implementation, which is carried out with a twenty node 3D brick element (Fig. 1) based on isoparametric formulation. According to isoparametric formulation, the displacements, geometry and electrical potential at instant t can be expressed in terms of their nodal parameters with the help of same interpolation functions (Bathe 1996) as

$${}^t x_i = \sum_{k=1}^{20} N^k(\xi, \eta, \zeta) {}^t x_i^k, \quad {}^t u_i = \sum_{k=1}^{20} N^k(\xi, \eta, \zeta) {}^t u_i^k, \quad {}^t\phi = \sum_{k=1}^{20} N^k(\xi, \eta, \zeta) {}^t\phi^k \tag{16}$$

where $N^k(\xi, \eta, \zeta)$ or simply N^k is the interpolation function corresponding to k-th node, while ${}^t x_i^k, {}^t u_i^k$ and ${}^t\phi^k$ are the coordinate, displacement and electrical potential at the corresponding node, respectively. In a similar manner, the incremental displacements and the incremental electrical potential ϕ can be expressed as

$$u_i = \sum_{k=1}^{20} N^k u_i^k \quad \text{and} \quad \phi = \sum_{k=1}^{20} N^k \phi^k \tag{17}$$

With the Eqs. (16) and (17), the incremental strain vectors $\{\overline{\varepsilon}^0\}$ and $\{\theta\}$ in (14) and incremental displacement vector $\{\overline{u}\}$ in (15) can be expressed in terms of incremental nodal displacement vector $\{\overline{U}\}$ and $\{\overline{\phi}\}$ (Manna *et al.* 2009).

Finally, with the help of Eqs. (14), (15), (16) and (17) after performing necessary rearrangement, the incremental equilibrium equation may be obtained in its final form as

$$[K_T]\{U\} = \{{}^{t+\Delta t}R\} - \{{}^{t+\Delta t}F\} - [M]\{{}^{t+\Delta t}\ddot{U}\} \tag{18}$$

where

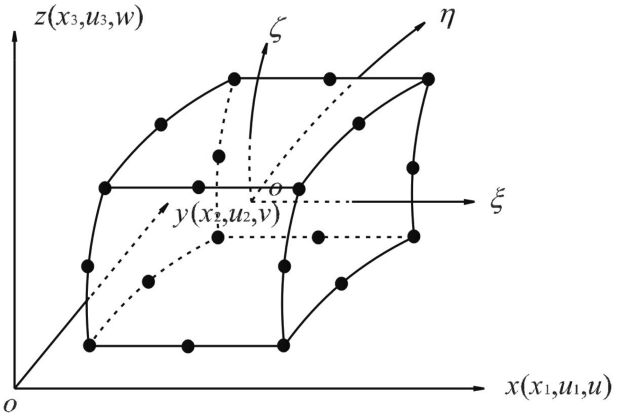

Fig. 1 Twenty-node 3D brick element

$$\{{}^{t+\Delta t}\ddot{U}\} = \begin{Bmatrix} \{{}^{t+\Delta t}\ddot{\overline{U}}\}^T \\ \{{}^{t+\Delta t}\ddot{\overline{\phi}}\}^T \end{Bmatrix} \tag{19}$$

$$\{U\} = \begin{Bmatrix} \{\overline{U}\}^T \\ \{\overline{\phi}\}^T \end{Bmatrix} \tag{20}$$

$$[M] = \int \begin{bmatrix} {}^t\rho N_u^T N_u & 0 \\ 0 & 0 \end{bmatrix} {}^t dV \tag{21}$$

$$[K_T] = \int \left(\begin{bmatrix} B_0 & 0 \\ 0 & B_\phi \end{bmatrix}^T [{}_t\overline{C}] \begin{bmatrix} B_0 & 0 \\ 0 & B_\phi \end{bmatrix} + \begin{bmatrix} B_G^T \, {}^t\overline{\tau} B_G & 0 \\ 0 & 0 \end{bmatrix} \right) {}^t dV \tag{22}$$

$$\{{}^{t+\Delta t}R\} = \int \begin{bmatrix} N_u^T & 0 \\ 0 & N_\phi^T \end{bmatrix} \begin{Bmatrix} {}^{t+\Delta t}_0\overline{t} \\ {}^{t+\Delta t}_0 Q \end{Bmatrix} {}^t dA \tag{23}$$

$$\{{}^{t+\Delta t}F\} = \int \begin{bmatrix} B_0 & 0 \\ 0 & B_\phi \end{bmatrix}^T \{{}^t\tau\} \, {}^t dV \tag{24}$$

Following the usual technique, one may carry out numerical integration involved in the above quantities according to Gauss quadrature integration rule where number of Gauss points taken is 3 in all the three directions. To get the solution of the time dependent incremental equilibrium Eq. (18), the direct time integration technique based on Newmark beta method (Bathe 1996) is used. Since the present problem involves geometric as well as material nonlinearities, it requires some iteration technique (Bathe 1996) to get the satisfaction of the equilibrium Eq. (18) within a specified tolerance. The rubber is a near incompressible hyperelastic material and its constitutive tensor ${}_t\overline{C}_{ijkl}$ is obtained from the strain energy density function W of Peng and Chang (1997), which is explained in Manna *et al*. (2009).

3. Results and discussions

In this section, numerical examples are solved by the finite element model developed in this study to demonstrate its capabilities. As there is no existing result for the dynamic response of rubber component with surface bonded piezoelectric patches/layers, the validation is done an example of a steel beam and a PVDF bimorph beam at the beginning. The model is then applied to dynamic response and its control of smart rubber cantilever beam.

3.1 A steel cantilever subjected to step transverse load at the free end

A steel cantilever beam having 100 mm length, 5 mm width and 1 mm thickness is subjected to a step point load of −5.0 N at mid-point of the free end of the cantilever beam. The step load is applied fully in two time steps. The linear and nonlinear dynamic response of the beam is evaluated by the present model and the time history of the tip deflection is presented in Fig. 2. In order to validate the present results, the beam is also analyzed by the commercial code ANSYS 8.0 and the results obtained are included in Fig. 2, which shows a close agreement between the results obtained from the two sources. The nonlinearity has given a stiffening effect as expected and it is reflected through reduction of maximum tip deflection value as well as reduction in the period of vibration. The Young's modulus (E), density (ρ) and Poisson's ratio (ν) of steel beam are taken as 197.0 GPa, 7.9×10^3 kg/m^3 and 0.33, respectively. The beam is modeled with 10 elements long the length, 1 element along the width and 2 elements along the depth (mesh: 10×1×2), and a time step (Δt) of 1.5×10^{-4} sec is taken for the time integration.

3.2 A PVDF bimorph cantilever beam subjected to axial and transverse step loads

The dynamic response of a bimorph cantilever beam made with two identical piezoelectric PVDF layers having same dimensions and polarity as shown in Fig. 3 is studied in this example. The beam is subjected distributed axial as well as transverse step load as shown in Fig. 4 where the total peak transverse load is −0.005 N and that is 0.1 N for the axial compressive load. Fig. 4 also shows the

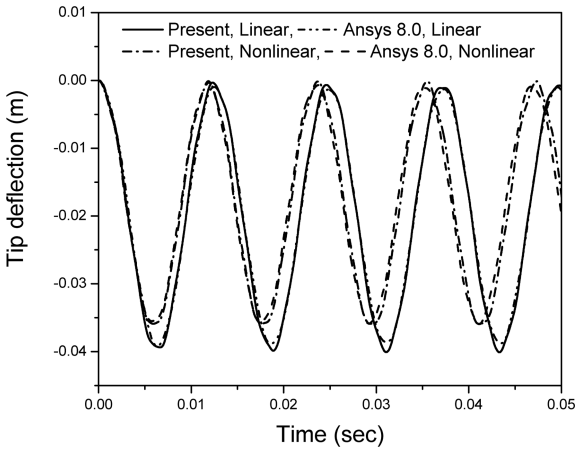

Fig. 2 Dynamic response of a steel cantilever beam

time variation of the loads where Δt_0 is taken as 0.002 sec, which is followed in an identical manner in the subsequent examples. With the material properties given in Table 1 for PVDF, the analysis of the beam is carried out with a mesh size of 10×1×2 using time step (Δt) of 0.001 sec. The time history for the deflection obtained at the tip of the cantilever bimorph beam and the voltage developed at the root of the beam are presented in Figs. 5 and 6, respectively along with those by Mukherjee and Chaudhuri (2005b). Apart from these results based on nonlinear analysis, the results based on linear analysis of Mukherjee and Chaudhuri (2005b) are also included in Figs. 5 and 6, which predicts a much smaller structural deformation and sensed voltage. In this case the nonlinearity gives softening effect due to the presence of axial compression.

The same bimorph cantilever beam is studied under identical condition except the magnitude of the transverse loads, which is taken as −0.025 N in the present case i.e., much larger than the previous case. The time history for the deflection at the tip of the beam and voltage developed at the root of the beam, obtained in linear as well as nonlinear analyses are presented in Figs. 7 and 8, respectively, which show a similar effect. However, the larger transverse load introduces larger

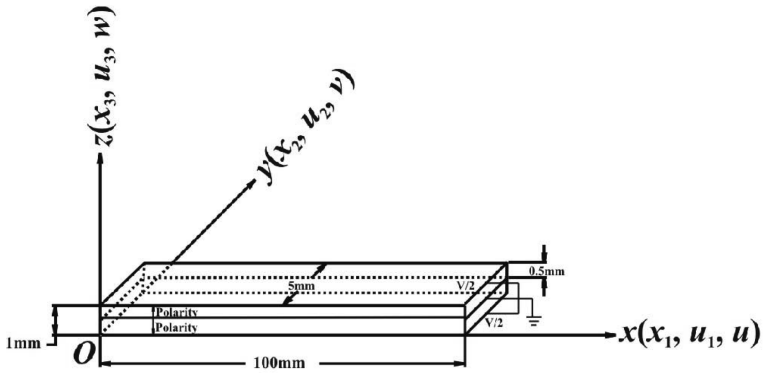

Fig. 3 PVDF bimorph cantilever beam

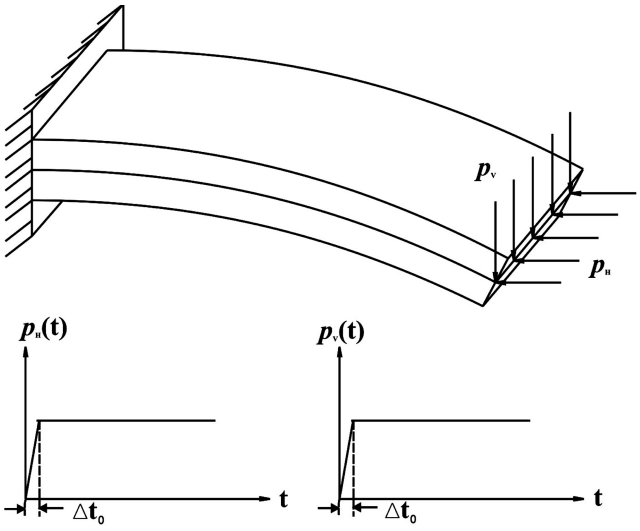

Fig. 4 Loads on the PVDF bimorph cantilever beam

Table 1 Material constants of piezoelectric material (PVDF) (Mukherjee and Chaudhuri 2005b)

Material	Material constants	
PVDF	Young's modulus, E (GPa)	2.0
	Poisson's ratio, ν	0.29
	Density, ρ (kg/m^3)	1800
	Piezoelectric stress coefficient, e_{31} (C/m^2)	0.046
	Dielectricity, L_3 (F/m)	1.062×10^{-10}
	Maximum operating voltage (V/μm)	30

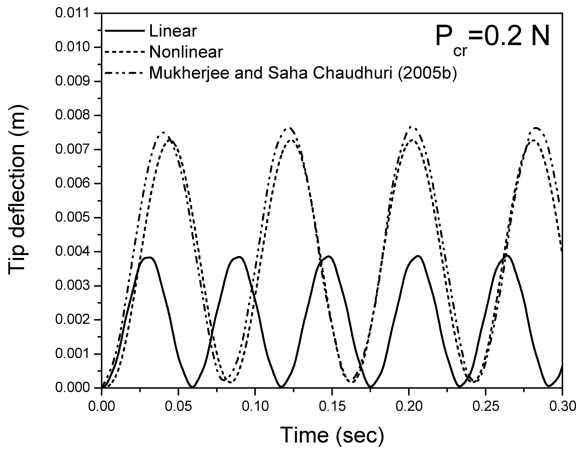

Fig. 5 Dynamic response (deflection) of the bimorph cantilever beam under transverse load of −0.005 N and axial compressive load of 0.1 N applied at the free end

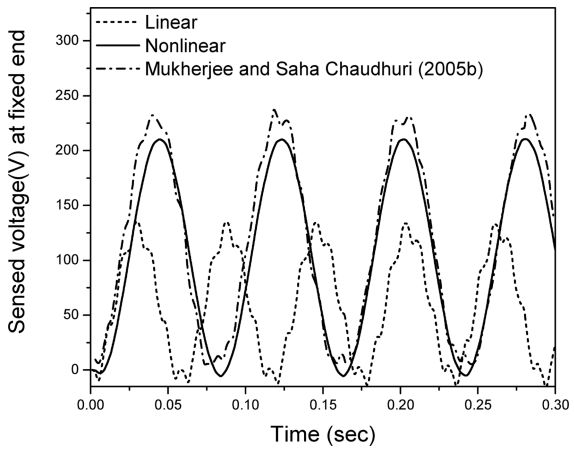

Fig. 6 Dynamic response (sensed voltage) of the bimorph cantilever beam under transverse load of −0.005 N and axial compressive load of 0.1 N applied at the free end

structural deformation as well as sensed voltage.

Again, the bimorph beam is studied with the transverse load of −0.025 N and without any axial load to see the nonlinear effect on the behaviour of the beam. The tip deflection and sensed voltage at the fixed end are plotted in Figs. 9 and 10, respectively, which show that the nonlinear effect on both deflection and sensed voltage is marginal. It has shown that presence of axial compressive force has imposed severe nonlinearity in the present bimorph beam.

The bimorph beam is once again analyzed with the loads used in the first case (−0.005 N of transverse load and 0.1 N of axial compressive load) taking a time step of 0.0005 sec. The analysis is carried out with feedback control taking gain G as 0 and 10. The tip deflection obtained in the nonlinear analysis is presented in Fig. 11 along with those obtained by Mukherjee and Chaudhuri (2005b) for validation. Fig. 11 shows that both the results agree well.

3.3 A rubber cantilever beam with surface-bonded piezoelectric layers under step load

The problem of a rubber cantilever beam having 100 mm length (L), 5 mm width (b) and 10 mm thickness (t_s) with a PVDF layer having 0.5 mm thickness (t_p) bonded on the top surface of the

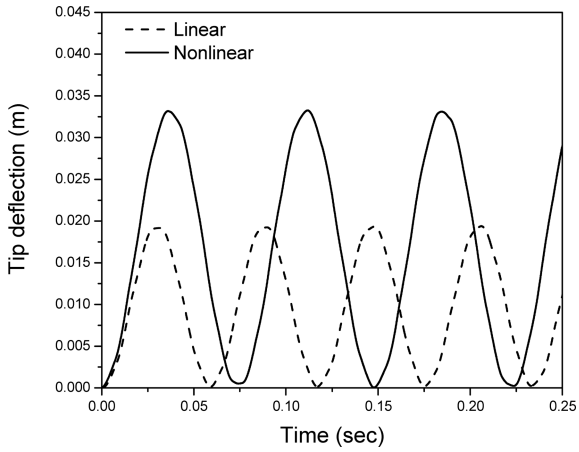

Fig. 7 Dynamic response (deflection) of the bimorph cantilever beam under transverse load of −0.025 N and axial compressive load of 0.1 N applied at the free end

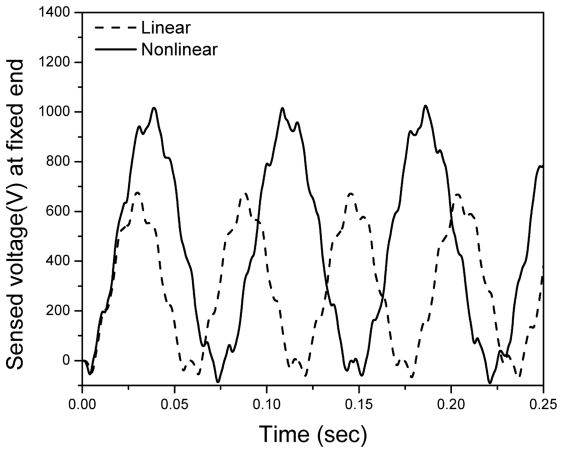

Fig. 8 Dynamic response (sensed voltage) of the bimorph cantilever beam under transverse load of −0.025 N and axial compressive load of 0.1 N applied at the free end

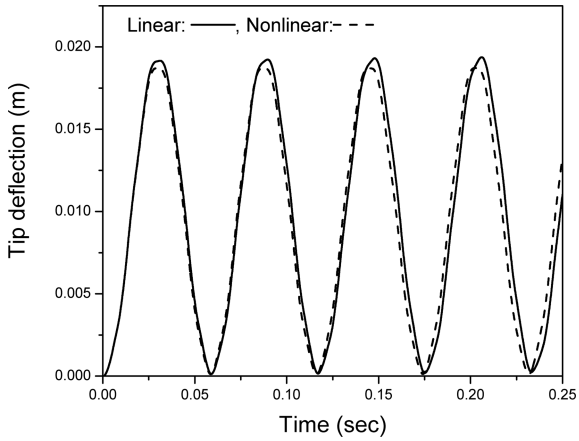

Fig. 9 Dynamic response (deflection) of the bimorph cantilever beam under transverse load of −0.025 N applied at the free end

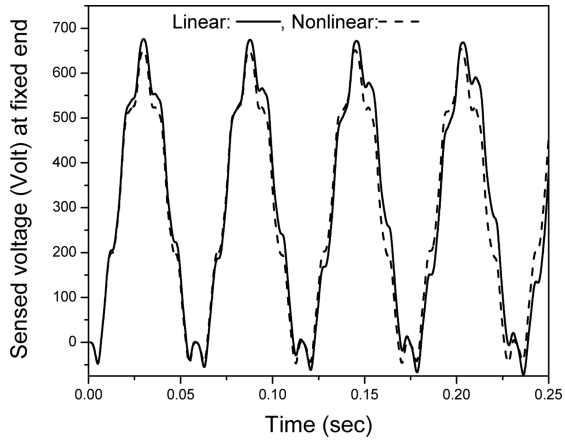

Fig. 10 Dynamic response (sensed voltage) of the bimorph cantilever beam under transverse load of −0.025 N applied at the free end

rubber beam as shown in Fig. 12 is studied in this example. The beam is subjected to a step point load (P_t) of 0.2 N acting at the point (Q) of the free end of the beam as shown in Fig. 12. The rubber material is modeled with the strain energy density function of Ogden-Tschoegl model (Peng and Chang 1997) taking different material properties as stated in Table 2. The density of the rubber layer is taken as 1.2×10^3 kg/m^3. The analysis is carried out with a time step of $\Delta t = 0.0015$ sec for the time integration where the rubber layer is divided into 120 elements (mesh size: 20×1×6) while the PVDF layer is divided into 20 elements (mesh size: 20×1×1). The time history for the deflection at point Q and the sensed voltage at point P (Fig. 12) due to direct piezoelectric effects obtained in the nonlinear as well as linear analysis are presented in Figs. 13 and 14, respectively. In the linear

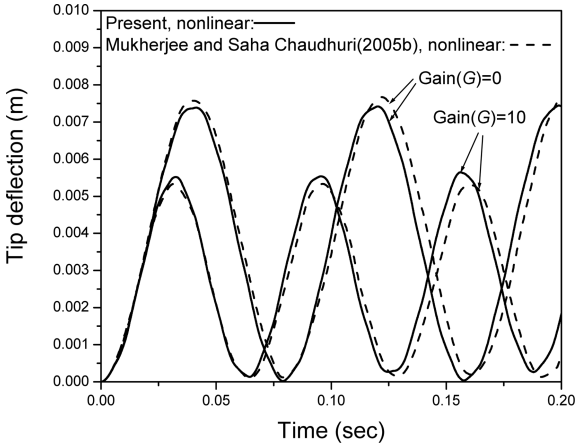

Fig. 11 Vibration control of the bimorph cantilever beam

analysis, the constitutive relation is taken at the undeformed state of the rubber layer. Figs. 13, 14 show that the geometric nonlinearity and possibly material nonlinearity to some extent of the rubber material jointly reduced the tip deflection and the sensed voltage at the root of the cantilever beam.

3.4 Vibration control of a smart rubber cantilever beam

The vibration control of a smart rubber beam is studied by three different potential feedback control schemes/simple feedback control schemes and it is observed that these schemes did not work well. So an attempt is made with a different scheme, known as velocity feedback control scheme, used in the study of Samanta *et al.* (1996), and it work well.

The smart rubber cantilever beam is 100 mm long, 5 mm wide and consists of 2.5 mm thick central rubber layer with two surface bonded PVDF layers each 0.5 mm thick used as sensor and actuator as shown in Fig. 15. The vibration control of the beam is studied using velocity feedback control scheme (Samanta *et al*. 1996) with the information of velocities at the nodes of the sensor. The rubber layer is divided into 160 elements (mesh size: 20×6×1) and each PVDF layer into 20 elements (mesh size: 20×1×1). The material of the rubber layer is modeled with the strain energy

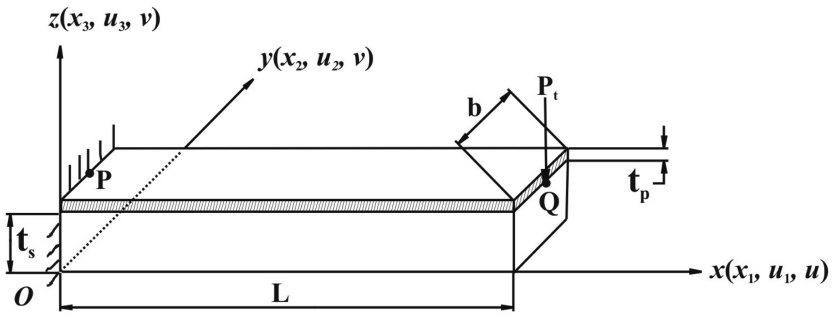

Fig. 12 A rubber cantilever beam with surface bonded piezoelectric layer

Table 2 Material constants of the different rubber material models

Material model	m	μ_1	μ_2	μ_3	α_1	α_2	α_3	ν
		(MPa)						
Neo-Hookean (NH)	1	0.3924	0.0	0.0	2.0	0.0	0.0	0.49932
Mooney-Rivlin (MR)	2	0.367	-0.0292	0.0	2.0	-2.0	0.0	0.49932
Ogden-Tschoegl (OT)	3	0.618	0.001245	-0.00982	1.3	5.0	-2.0	0.49932

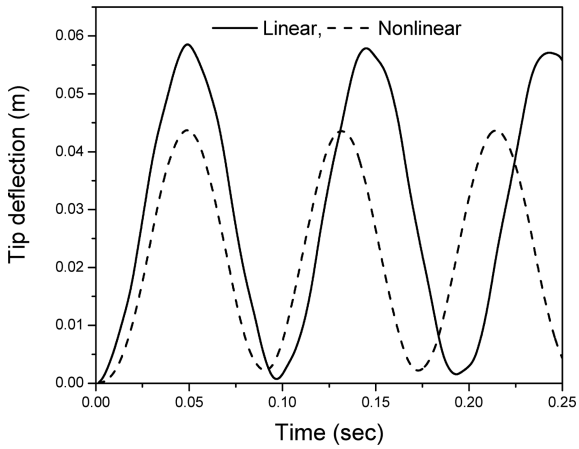

Fig. 13 Time history of the deflection at the tip of the rubber cantilever beam with surface bonded PVDF sensor layer

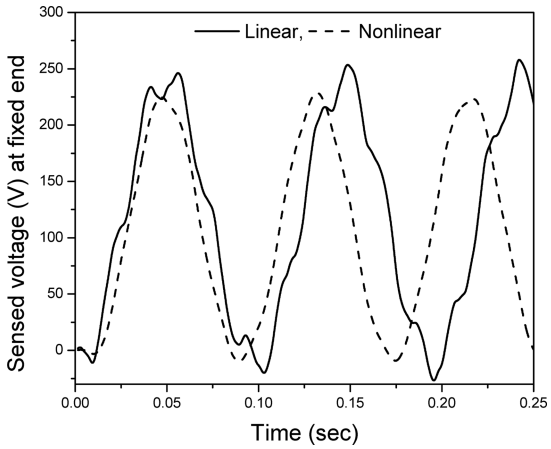

Fig. 14 Time history of the sensed voltages at the root of the rubber cantilever beam with surface bonded PVDF sensor layer

density function of Ogden-Tschoegl. The density of natural rubber material (1.2×10^3 kg/m^3) is used. A vertically downward point load of 0.025 N is suddenly applied at the midpoint of the rubber top PVDF layer interface at the free end of the beam. The load is suddenly removed at an instant 0.0175 sec after its application. The time step (Δt) used for time integration is 7.0×10^{-4} sec. The value of the charge amplifier gain (G_c) is taken as $3.98\times10^2\ \Omega$ and the gain factor (G) of the controller is taken as 0 and 10. The tip deflection of the beam and the sensed voltage in the senor at fixed end of the beam are plotted against time in Figs. 16 and 17, respectively. It is found that the variation of tip deflection across the thickness direction of the beam is insignificant. It is observed from the figures that the velocity feedback control has gradually reduced the amplitude of vibration of the beam and consequently the sensed voltage in the sensor. It should be mentioned that any structural damping or viscoelastic damping of the rubber is not considered so far. Time rate of amplitude decay at larger gain value will be higher. Hence the beam reaches the undeformed state (tip deflection is zero) earlier. Thus the settling time in this case is much less.

A similar example of the cantilever smart rubber beam (Fig. 15) with different dimensions is studied to see effect of material nonlinearity of the rubber layer. The rubber layer is 1000 mm long, 50 mm wide and 25 mm thick while each PVDF layer has same thickness (0.5 mm) as used in the previous case. The analysis is carried out with same mesh size taking time step of 0.02 sec for the time integration. In order to observe the effect of material nonlinearity of the rubber layer, the

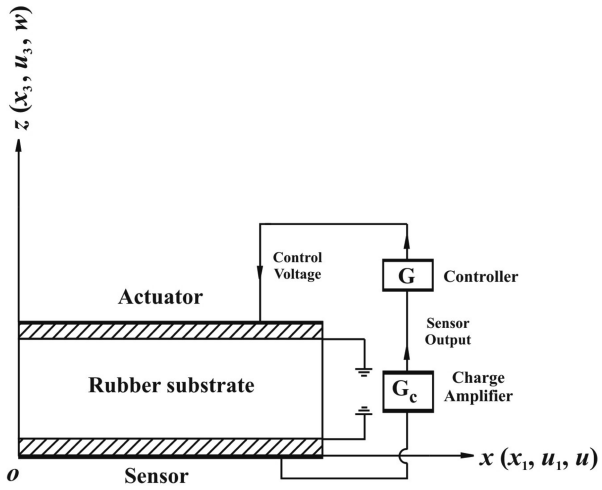

Fig. 15 Control arrangement of the cantilever smart rubber beam

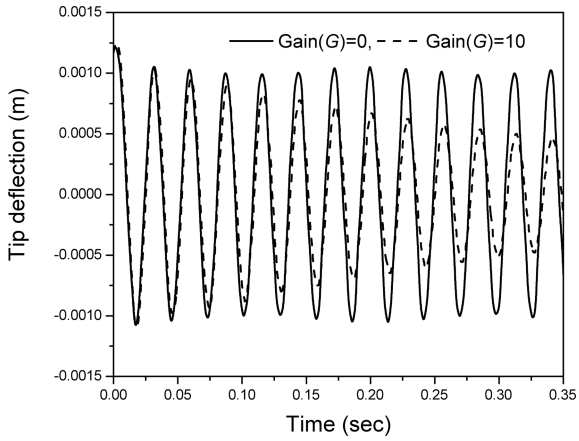

Fig. 16 Dynamic response (tip deflection) of the cantilever smart rubber beam

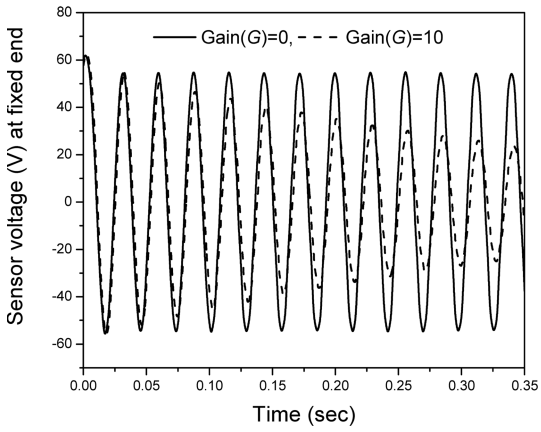

Fig. 17 Dynamic response (sensed voltage at fixed end) of the cantilever smart rubber beam

analysis is carried out with hyperelastic/nonlinear material behaviour as well as linear material behaviour where the constitutive tensor is taken corresponding to undeformed state of the rubber material. The geometric nonlinearities is taken in both the cases. The beam is subjected a suddenly applied point load of 0.25 N in a similar as that of the previous case. The load is removed after 25 time steps when a linear material behaviour is taken for the rubber while it 20 time steps in the other case. The velocity feedback control scheme is activated after the removal of the load. All other things are identical to those taken in the previous one. The tip deflection and sensed voltage in the sensor at the fixed end obtained in the present analysis are plotted against time in Figs. 18 and 19, respectively. Fig. 18 shows that the material nonlinearity of rubber layer has reduced the vibration amplitude of tip deflections for both $G = 0$ and 10. A similar behavior is observed in the sensed voltage plotted in Fig. 19.

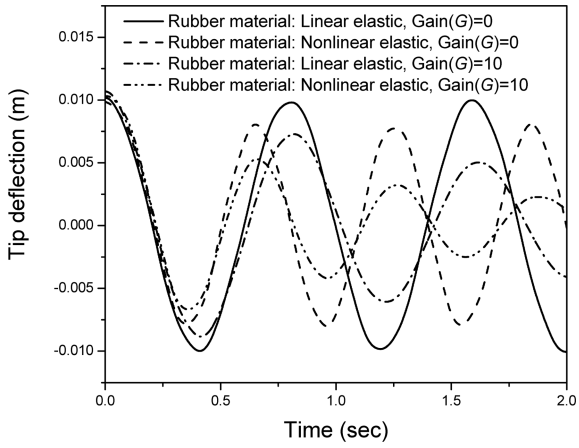

Fig. 18 Dynamic response (tip deflection) of the smart hyperelastic (OT model) rubber cantilever beam under a step tip point load of −0.25 N

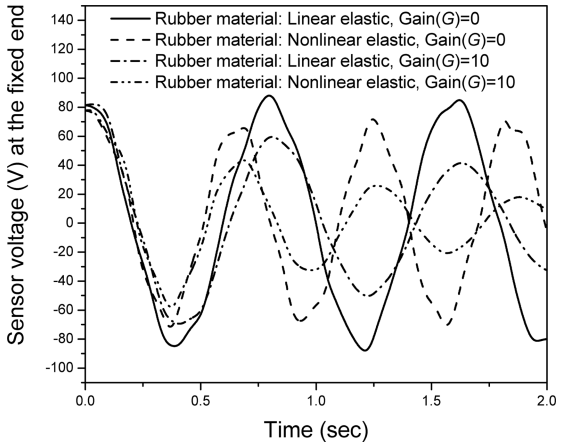

Fig. 19 Dynamic response (sensed voltage at the fixed end) of the smart hyperelastic (OT model) rubber cantilever beam under a step tip point load of −0.25 N

4. Conclusions

A finite element model based on updated Lagrangian approach is proposed for nonlinear dynamic response and its control of rubber components with surface bonded piezoelectric layers under different loading conditions. A compressible stain energy function is used to get the constitutive matrix of the near incompressible hyperelastic rubber material. A twenty-node solid brick element is used to implement the present formulate. The present model is applied to a PVDF bimorph beam subject to a combination of transverse and compressive forces to validate the present formulation. The results predicted by the present model agreed well with the available published results. The model is then applied to a smart rubber beam comprising piezoelectric (PVDF) and rubber layers under transverse and compressive axial forces is considered to show the spring stiffening and softening effects of piezoelectric material. Finally, a cantilever smart rubber beam is investigated to show how the piezoelectric materials are uilized to control the structural deformations using potential feedback control schemes/simple feedback control schemes and velocity feedback control schemes. It is observed that the velocity feedback control scheme is more effective in the present problem. The present method gives a straightforward and simple approach for the nonlinear analysis of rubber components with piezoelectric patches.

References

Allik, H. and Hughes, T.J. (1970), "Finite element method for piezoelectric vibration", *Int. J. Numer. Meth. Eng.*, **2**, 151-157.

Austin, E.M. and Ananthasayanam, B. (2002), "Modeling of piezoelectric materials on rubber beams", *Proc. SPIE,* **4697**, 131-138.

Bailey, T. and Hubbard, J.E. (1985), "Distributed piezoelectric-polymer active vibration control of a cantilever beam", *J. Guid. Control Dynam.,* **8**(5), 605-611.

Bathe, K.J. (1996), *Finite Element Procedures in Engineering Analysis*, Prentice Hall, Englewood Cliffs.
Chattopadhyay, A., Kim, H.S. and Ghosal, A. (2004), "Non-linear vibration analysis of smart composite structures with discrete delamination using a refined layerwise theory", *J. Sound Vib.*, **273**(1-2), 387-407.
Chen, S.H., Wang, Z.D. and Liu, X.H. (1997), "Active vibration control and suppression for intelligent structures", *J. Sound Vib.*, **200**(2), 167-177.
Crawley, E.F. and de Luis, J. (1987), "Use of piezoelectric actuators as elements of intelligent structures", *AIAA J.*, **25**(10), 1373-1385.
Fanson, J.L. and Caughey, T.K. (1987), "Positive position feedback control for large space structures", *Proceedings of the 28th AIAA/ASME/ASCE/AHS/ASC Structures, Structural Dynamics and Material Conference*, Monterey, California, USA.
Forward, R. (1979), "Electronic damping of vibrations in optical structures", *Appl. Optic*s, **18**(5), 690-697.
Gaudenzi, P., Carbonaro, R. and Benzi, E. (2000), "Control of beam vibrations by means of piezoelectric devices: theory and experiments", *Compos. Struct.*, **50**(4), 373-379.
Gent, A.N. (2001), *Engineering with Rubber*, 2nd Ed., Hanser Publishers.
Lee, S.J., Reddy, J.N. and Rostam-Abadi, F. (2004), "Transient analysis of laminated composite plates with embedded smart-material layers", *Finite Elem. Anal. Des.*, **40**(5-6), 463-483.
Lim, C.W., He, L.H. and Soh, A.K. (2001), "Three-dimensional electromechanical responses of a parallel piezoelectric bimorph", *Int. J. Solids Struct.*, **38**, 2833-2849.
Manna, M.C., Sheikh, A.H. and Bhattacharyya, R. (2009), "Static analysis of rubber components with piezoelectric patches using nonlinear finite element", *Smart Struct. Syst.,* **5**(1), 23-42.
Mukherjee, A. and Chaudhuri, A.S. (2004), "Exact solutions for instability control of piezolaminated imperfect struts", *AIAA J.,* **42**(4), 857-859.
Mukherjee, A. and Chaudhuri, A.S. (2005a), "Active control of piezolaminated columns – exact solutions and experimental validation", *Smart Mater. Struct.,* **14**, 475-482.
Mukherjee, A. and Chaudhuri, A.S. (2005b), "Nonlinear dynamic response of piezoelectric smart beams", *Comput. Struct.*, **83**, 1298-1304.
Newmark, N.M. (1959), "A method of computation for structural dynamics", *J. Eng. Mech. Div. ASCE*, **85**, 67-94.
Ogden, R.W. (1984), *Non-linear Elastic Deformations*, Ellis Horwood, Chichester.
Olson, H.F. (1956), "Electronic control of noise, vibration, and reverberation", *J. Acoust. Soc. Am.*, **28**, 966-972.
Park, C. and Chopra, I. (1996), "Modeling piezoceramic actuation of beams in torsion", *AIAA J.*, **34**(12), 2582-2589.
Peng, S.H. and Chang, W.V. (1997), "A compressible approach in finite element analysis of rubber-elastic materials", *Comput. Struct.*, **62**, 573-593.
Ray, M.C., Bhattacharyya, R. and Samanta, B. (1993), "Exact solution for static analysis of intelligent structures", *AIAA J.*, **31**(9), 1684-1691.
Ray, M.C., Bhattacharyya, R. and Samanta, B. (1994), "Static analysis of an intelligent structure by the finite element method", *Comput. Struct.*, **52**(4), 617-631.
Ray, M.C., Bhattacharyya, R. and Samanta, B. (1998), "Exact solutions for dynamic analysis of composite plates with distributed piezoelectric layers", *Comput. Struct.*, **66**(6), 737-743.
Samanta, B., Ray, M.C. and Bhattacharyya, R. (1996), "Finite element model for active control of intelligent structures", *AIAA J.*, **34**(9), 1885-1893.
Thornburgh, R.P., Chattopadhyay, A. and Ghosal, A. (2004), "Transient vibration of smart structures using a coupled piezoelectric-mechanical theory", *J. Sound Vib.*, **274**(1-2), 53-72.
Tiersten, H.F. (1969), *Linear Piezoelectric Plate Vibrations*, 1st Ed., Plenum Press, New York.
Ye, S., Ling, S.F. and Ying, M. (2000), "Large deformation finite element analyses of composite structures integrated with piezoelectric sensors and actuators", *Finite Elem. Anal. Des.*, **35**, 1-15.

CC